

# Lifetimes and $g$ -factors of the HFS states in H-like and Li-like bismuth

Volker Hannen<sup>1</sup>, Jonas Vollbrecht<sup>1</sup>, Zoran Andelkovic<sup>2</sup>,  
Carsten Brandau<sup>2,3</sup>, Andreas Dax<sup>4</sup>, Wolfgang Geithner<sup>2</sup>,  
Christopher Geppert<sup>5,6</sup>, Christian Gorges<sup>5,6</sup>,  
Michael Hammen<sup>6,7</sup>, Simon Kaufmann<sup>5</sup>, Kristian König<sup>5</sup>,  
Yuri A. Litvinov<sup>2</sup>, Matthias Lochmann<sup>5</sup>, Bernhard Maaß<sup>5</sup>,  
Johann Meisner<sup>8</sup>, Tobias Murböck<sup>9</sup>, Rodolfo Sánchez<sup>2</sup>,  
Matthias Schmidt<sup>8</sup>, Stefan Schmidt<sup>5</sup>, Markus Steck<sup>2</sup>,  
Thomas Stöhlker<sup>2,10,11</sup>, Richard C. Thompson<sup>12</sup>,  
Christian Trageser<sup>3</sup>, Johannes Ullmann<sup>1,5</sup>,  
Christian Weinheimer<sup>1</sup> and Wilfried Nörtershäuser<sup>5</sup>

<sup>1</sup>Institut für Kernphysik, Westfälische Wilhelms-Universität Münster, Germany

<sup>2</sup>GSI Helmholtzzentrum für Schwerionenforschung, Darmstadt, Germany

<sup>3</sup>I. Physikalisches Institut, Justus-Liebig-Universität Gießen, Germany

<sup>4</sup>Paul Scherrer Institut, Villigen, Switzerland

<sup>5</sup>Institut für Kernphysik, Technische Universität, Darmstadt, Germany

<sup>6</sup>Institut für Kernchemie, Johannes Gutenberg-Universität Mainz, Germany

<sup>7</sup>Helmholtz Institut Mainz, Johannes Gutenberg-Universität Mainz, Germany

<sup>8</sup>Physikalisch-Technische Bundesanstalt, Braunschweig, Germany

<sup>9</sup>Institut für Angewandte Physik, Technische Universität Darmstadt, Germany

<sup>10</sup>Helmholtz Institut Jena, Germany

<sup>11</sup>Institut für Optik und Quantenelektronik, Jena, Germany.

<sup>12</sup>QOLS Group, Department of Physics, Imperial College London, London, UK.

E-mail: hannen@uni-muenster.de

**Abstract.** The LIBELLE experiment performed at the experimental storage ring (ESR) at the GSI Helmholtz Center for Heavy Ion Research in Darmstadt, Germany, has successfully determined the ground state hyperfine (HFS) splittings in hydrogen-like ( $^{209}\text{Bi}^{82+}$ ) and lithium-like ( $^{209}\text{Bi}^{80+}$ ) bismuth. The study of HFS transitions in highly charged ions enables precision tests of QED in extreme electric and magnetic fields otherwise not attainable in laboratory experiments. Besides the transition wavelengths the time resolved detection of fluorescence photons following the excitation of the ions by a pulsed laser system also allows to extract lifetimes of the upper HFS levels and  $g$ -factors of the bound  $1s$  and  $2s$  electrons for both charge states. While the lifetime of the upper HFS state in  $^{209}\text{Bi}^{82+}$  has already been measured in earlier experiments, an experimental value for lifetime of this state in  $^{209}\text{Bi}^{80+}$  is reported for the first time in this work.

*Keywords:* Highly charged ions, hyperfine transitions, lifetimes

## 1. Introduction

Highly charged ions provide a testing ground for QED calculations in extreme electric (up to  $10^{16}$  V/cm) and magnetic (up to  $10^4$  T) fields [1, 2] that cannot be created in the laboratory with conventional methods (like lasers and superconducting magnets). Especially interesting in this context is the study of hyperfine transitions in hydrogen-like and lithium-like ions. By taking the so-called specific difference [3] of the HFS splittings of both charge states, it is possible to cancel nuclear-structure effects (most notably the Bohr-Weisskopf effect caused by the nuclear magnetization distribution) whose uncertainty would otherwise obscure the QED corrections under study. The LIBELLE<sup>‡</sup> experiment was for the first time able to measure H-like and Li-like HFS splittings in the same isotope [4] with sufficient precision to allow for a test of bound state QED calculations. While the prime target of the experiment was the determination of the transition energies, the time-resolved acquisition of the fluorescence photons emitted during the de-excitation of the ions also allowed to extract lifetimes of the upper HFS states and, together with the measured transition energies, to calculate  $g$ -factors of the bound  $1s$  electron for H-like bismuth and of the  $2s$  electron for Li-like bismuth. The following sections will provide details on the experimental procedure and analysis of the data required to extract the aforementioned quantities.

## 2. LIBELLE Experiment

The experimental setup of the LIBELLE Experiment has been explained in detail in several publications [4, 5, 6, 7, 8, 9, 10] with a focus on the extraction of the wavelengths of the H-like and Li-like HFS transitions. The experiment proceeded in two incarnations with an initial beam-time in 2011 that succeeded for the first time to observe the ground state HFS transition in Li-like bismuth in a laser spectroscopy experiment and a second beam-time in 2014 that featured a greatly increased accuracy in the determination of the level splittings by continuously monitoring the electron cooler voltage with a high-precision HV divider provided by the National Metrology Institute of Germany (PTB) and an improved DAQ system that also allowed to obtain high statistics data on the lifetime of the two HFS states.

Figure 1 gives an overview of the experimental setup. In the experiment two bunches of either H-like ( $^{209}\text{Bi}^{82+}$ ) or Li-like ( $^{209}\text{Bi}^{80+}$ ) ions are revolving in the Experimental Storage Ring (ESR), located at the GSI facility, at a velocity of  $\beta \approx 0.71$ . The ion bunches are created after the injection of ions into the ring using a radio frequency (RF)-cavity operated at the second harmonic of the revolution frequency ( $\approx 2$  MHz) with a nominal amplitude of 500 V. The stored ions are cooled by means of an electron cooler operated at a voltage near -214 kV. A tunable pulsed laser system with a repetition rate of 30 Hz is synchronized with the revolution frequency of the ions and used to illuminate one of the two bunches (called 'signal' bunch in the following). The other ion bunch

<sup>‡</sup> **L**i ium-like **B**ismuth **E**xcitation by **L**aser **L**ight at the **E**SR |

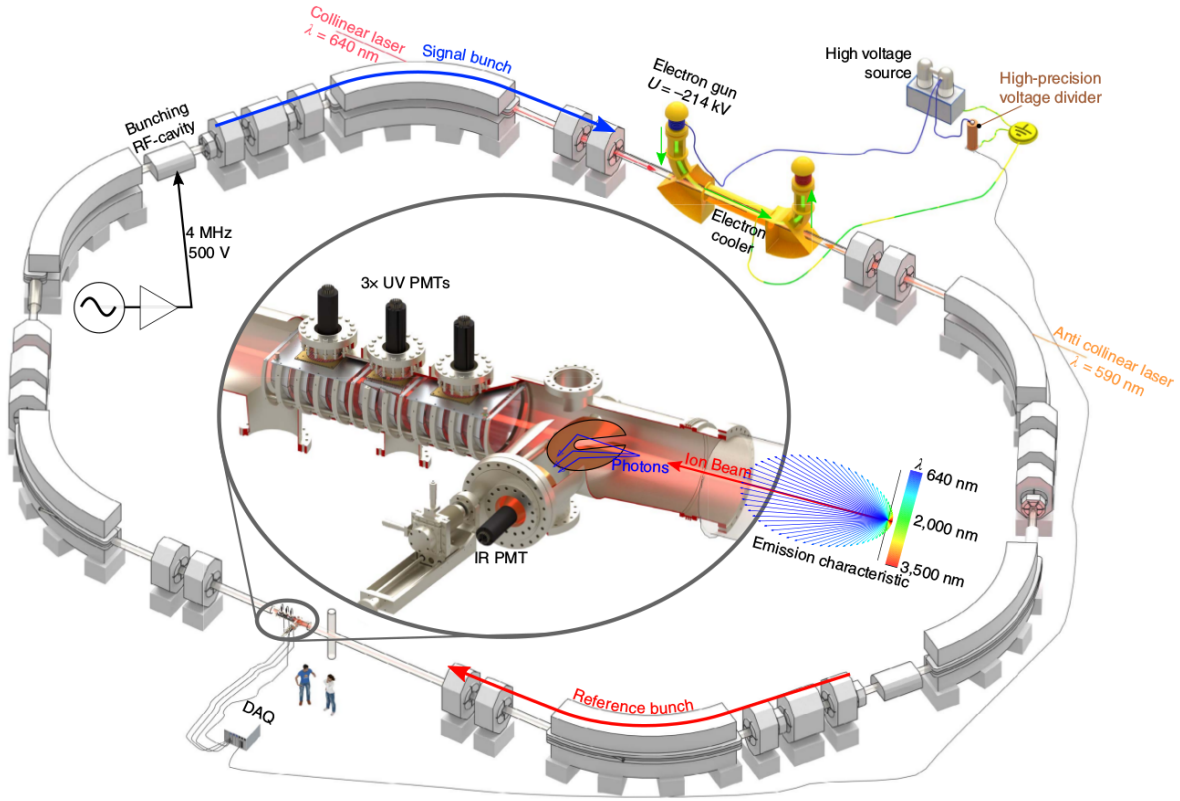


**Figure 1.** Schematic view of the LIBELLE experiment at ESR (reprinted from [4] with permission).

(called 'reference' bunch) is not illuminated and used to determine the experimental background.

For H-like bismuth the laser beam is injected in a counter propagating manner, shifting the wavelength of the laser from 590 nm in the laboratory system to 244 nm wavelengths in the rest-frame of the stored ions. Correctly tuned, the laser will excite the ions to the upper HFS state from which they will subsequently decay with a mean lifetime of about  $567 \mu\text{s}$  [11, 12] in the laboratory system. As the lifetime is long compared to the revolution period of the ions in the ring, fluorescence photons from the de-excitation are created along the whole circumference of the ESR and can therefore also be detected on the opposite side of the storage ring, using a suitable mirror system and photomultipliers (PMTs) situated on top of UV transparent windows in the beam-line (leftmost 3 PMTs visible in the inset of figure 1) [13, 5].

For Li-like bismuth the laser beam is injected in a co-propagating manner, shifting the wavelength of the laser from 640 nm in the laboratory system to 1554 nm wavelengths in the rest-frame of the stored ions. The theoretically predicted lifetime of the  $F = 5$  state in  $^{209}\text{Bi}^{80+}$  of about 118 ms [14] at  $\beta = 0.71$  is even longer and allows us again to detect fluorescence photons opposite to the electron cooler after resonant excitation with the laser. For that purpose a specially developed movable parabolic mirror system [15] (see right part of inlay in figure 1) has been used. The need to develop a special

detection system for the Li-like transition arises from the low signal rate connected to the long lifetime of the state and the long wavelength of the fluorescence photons that are outside the sensitive range of most PMTs. It is thus necessary to collect the most forward emitted photons that undergo the largest Doppler shift to shorter wavelengths and at the same time make use of the Lorentz boost of the emission characteristics to smaller polar angles.

### 3. Lifetime measurement

Besides the transition wavelengths the time resolved detection of the fluorescence photons following the excitation of the ions by the pulsed laser system allows to extract the lifetimes of the upper HFS states in both  $^{209}\text{Bi}^{82+}$  and  $^{209}\text{Bi}^{80+}$ .

#### 3.1. Method

For that purpose, the laser is fixed to the resonance wavelength and the rate of fluorescence photons is measured as a function of time after the laser pulses. While the time interval of 33.3 ms between individual laser pulses is sufficiently long for the excited HFS state in H-like bismuth to decay completely, the longer lifetime of the upper HFS state in Li-like Bi of about 118 ms at  $\beta = 0.71$  requires a shutter system to periodically block the laser for several lifetimes and therefore be able to observe a sufficiently large part of the decay curve to obtain a good fit of the lifetime in the laboratory system  $\tau_{\text{lab}}$ .

For the analysis the acquired signals are accumulated in timing bins with a width of  $25\text{ }\mu\text{s}$  for H-like ions and 5 ms for Li-like ions. For each of these bins, histograms of the number of counts as a function of time synchronized to the revolution period of the ions are extracted (see figure 2, left plot). In such a display, signals from the two

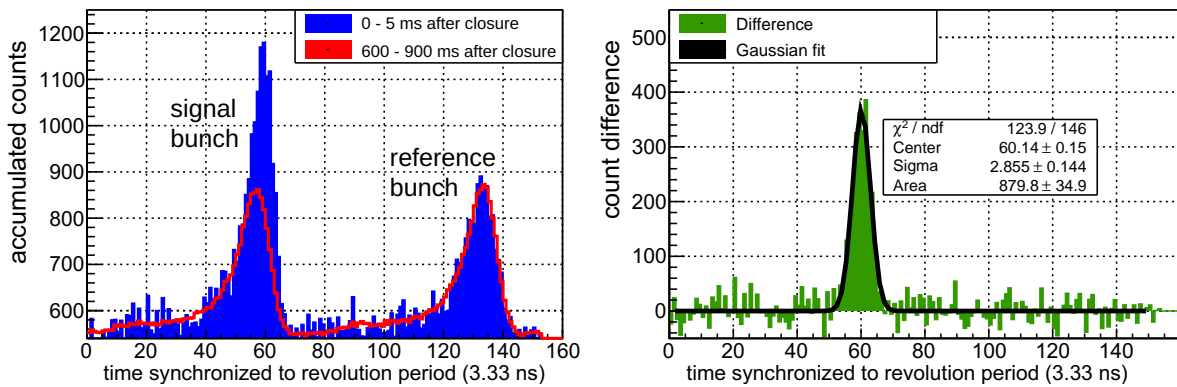


**Figure 2.** Left, blue histogram: signal and reference peaks for the HFS transition in Li-like bismuth accumulated during the first 5 ms after shutter closure. The red curve in the plot corresponds to the situation near the end of the decay interval averaged between 600 ms and 900 ms. Right: difference of the two histograms shown on the left, fitted with a Gaussian function.

ion bunches appear as peaks with one-sided tails resulting from an afterglow of excited rest-gas molecules after passage of the bunches. The bin width of these histograms is given by the time resolution of the time-to-digital converter (TDC) which operates with a 300 MHz clock. The left hand side of figure 2 shows in blue the accumulated counts for Li-like ions during the first 5 ms after excitation by the laser on resonance and subsequent closure of the shutter system. The signal peak (left) clearly exhibits a significantly higher number of events caused by fluorescence from the decay of the excited ions together with background processes, while the reference peak (right) contains background events only. Several lifetimes after shutter closure, practically all HFS states have decayed and signal and reference peaks now both exhibit roughly the same number of background counts (red curve, averaged over an interval between 600 ms and 900 ms). The right hand side in figure 2 displays the difference of the blue and red histograms that corresponds to photons from the HFS transitions only. This plot allows to determine the center and width of the fluorescence signal contribution to the overall event display.

To extract lifetime curves of the HFS transitions from the bunch histograms obtained for each time bin, the most robust method turned out to be a summation of the signal peak in a  $\pm n\sigma$  interval around the center of the signal count distribution determined as described above [16]. No background subtraction is performed in the process as especially for the parts of the lifetime curves where most HFS states have already decayed, one deals with the subtraction of two similarly large numbers that only leads to an increase in the statistical uncertainty of the extracted signal counts. Instead the background counts are summed together with the HFS signals and lead to a constant offset in the extracted lifetime curves that is treated as a fit parameter in the subsequent analysis. Figure 3 displays an example for such a lifetime curve obtained with Li-like bismuth ions. The number of counts is plotted against the time after closure of the

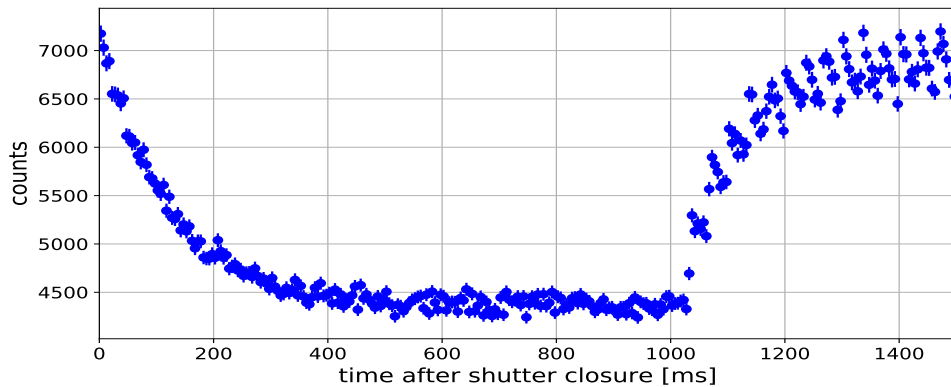


**Figure 3.** Fluorescence signal observed from Li-like bismuth ( $^{209}\text{Bi}^{80+}$ ) after resonant excitation of the M1 HFS transition. The shutter to the laser system is re-opened around 1000 ms after closure.

shutter required due to the long decay time in the case of Li-like bismuth. In the first 1000 ms one observes the expected exponential decay of the signal rate together with a constant offset from background events. Following that, the shutter is opened for 500 ms

such that the upper HFS state can be populated again by the laser. The displayed data is accumulated over many shutter cycles to obtain sufficiently high statistics. The shutter cycle is synchronized to the timing of the laser pulses and the pulse structure of the laser with 33.3 ms period can therefore be observed in the rising branch of the data when the shutter is open.

### 3.2. Fit model

While fitting lifetime data from the measurements with H-like bismuth ions is straightforward as one is dealing with a simple exponential decay plus background, more effort is required in the Li-like case, where one would also like to extract the information contained in the rising branch of the curve, during which the upper HFS state is gradually repopulated by a number of subsequent resonant laser pulses. The fit-model for the latter case has to take into account the processes of excitation, stimulated emission and spontaneous emission. The rate equation for the population of the upper HFS state  $N_2(t)$  reads:

$$\dot{N}_2(t) = N_1(t) B_{12} u - N_2(t) B_{21} u - N_2(t) A_{21} , \quad (1)$$

with the Einstein coefficients

$$A_{21} = \frac{1}{\tau} \quad B_{21} = A_{21} \frac{\lambda^3}{8\pi h} \quad g_1 B_{12} = g_2 B_{21} . \quad (2)$$

The coefficient for spontaneous emission  $A_{21}$  is the inverse of the mean lifetime  $\tau$ .  $g_1$  and  $g_2$  are the number of magnetic sub-states of the ground state ( $F = 4$ ) and the excited state ( $F = 5$ ) of the given HFS transition.  $N_1(t)$ ,  $N_2(t)$  are the occupation numbers of the respective state, which yield the total number of stored ions  $N$  via  $N = N_1(t) + N_2(t)$ . As the typical storage time of the ions in the ring was about 20 minutes, the time dependence of the total ion number over the timescale of a single 1,5 s shutter cycle can be neglected.  $\lambda$  denotes the wavelength of the transition and  $u$  the time averaged spectral energy density of the laser. Equation 1 can be re-written as follows:

$$\dot{N}_2(t) = \left\{ \frac{g_2}{g_1} N - \left( \frac{g_2}{g_1} + 1 \right) N_2(t) \right\} \frac{\lambda^3 u}{8\pi h} \frac{1}{\tau} - N_2(t) \frac{1}{\tau} \quad (3)$$

With the abbreviation  $\phi := \frac{\lambda^3 u}{8\pi h}$  eq. 3 simplifies to

$$\dot{N}_2(t) = \underbrace{\frac{g_2}{g_1} N \frac{\phi}{\tau}}_{:= a} - \underbrace{\left( \frac{\left( \frac{g_2}{g_1} + 1 \right) \phi + 1}{\tau} \right)}_{:= b} N_2(t) = a - b N_2(t) \quad (4)$$

The differential equation 4 can be solved using the ansatz  $N_2(t) = \frac{a}{b} + c e^{-bt}$ , where  $c$  is a constant, introduced by the boundary conditions at  $t = 0$  and is therefore given by  $c = N_2(0) - \frac{a}{b}$ . Together it yields

$$N_2(t) = \frac{a}{b} + \left( N_2(0) - \frac{a}{b} \right) \exp(-bt) \quad (5)$$

Stimulated emission as well as excitation do not take place during the full measurement interval since the laser is blocked for a defined time. Therefore a distinction is needed, with the two cases

- (i)  $t \leq t_c$ : The laser is blocked, therefore only spontaneous emission takes place
- (ii)  $t > t_c$ : The ions are excited by the the laser and all three processes are taken into account

The corresponding fit function is given by

$$f(t) = \begin{cases} s \cdot N_2(0) \exp\left(-\frac{t}{\tau}\right) + d & \text{for } t \leq t_c \\ s \cdot \left[\frac{a}{b} + \left(N_2(t_c) - \frac{a}{b}\right) \exp(-b(t - t_c))\right] + d & \text{for } t > t_c, \end{cases} \quad (6)$$

where  $d$  accounts for a constant background and  $s$  is a scaling factor representing further experimental parameters like measurement time and observed solid angle. Equation 6 holds for excitation with a continuous laser beam and does not yet take into account the pulse structure of the laser. Therefore a further modification of the model has been implemented in the fitting code, taking into account that during the rising branch of the lifetime curve only each 6th or 7th bin actually contains a laser shot.

### 3.3. Beam-time 2014

The main part of the LIBELLE beam-time in 2014 was spent on the precise determination of the wavelengths of the HFS transitions in  $^{209}\text{Bi}^{82+}$  and  $^{209}\text{Bi}^{80+}$ . For that purpose the laser wavelength was scanned repeatedly across the respective transitions and a number of dedicated systematics measurements, among others investigating the influence of the electron cooler current or the buncher amplitude on the observed transition wavelength, were performed [4, 5]. In addition to this, some runs were recorded in which the laser was fixed to the transition wavelength of either  $^{209}\text{Bi}^{82+}$  or  $^{209}\text{Bi}^{80+}$  (in the latter case with the optical shutter system in operation) to obtain high statistics data on the lifetime of the states.

*Li-like bismuth* After the first half of the beam-time it was discovered that one of the drift-electrodes inside the electron cooler was not properly connected leading to fluctuations in the revolution frequency of the ion bunches that were then compensated by adapting the electron cooler voltage. After the electrode had been properly grounded, these fluctuations disappeared. At the same time however, the experimental background in the fluorescence detection increased, possibly due to a slight change in the beam properties following the repair action. We therefore collect the lifetime measurements for the HFS transition in Li-like bismuth in two datasets, one before and one after the maintenance of the electrode. Figure 4 displays the respective datasets together with results from the fit. The reduced  $\chi^2$ -values of both fits are consistent with one indicating that the model provides an adequate description of the data. The residuals do not show any non-statistical fluctuations and follow a Gaussian distribution around zero. The

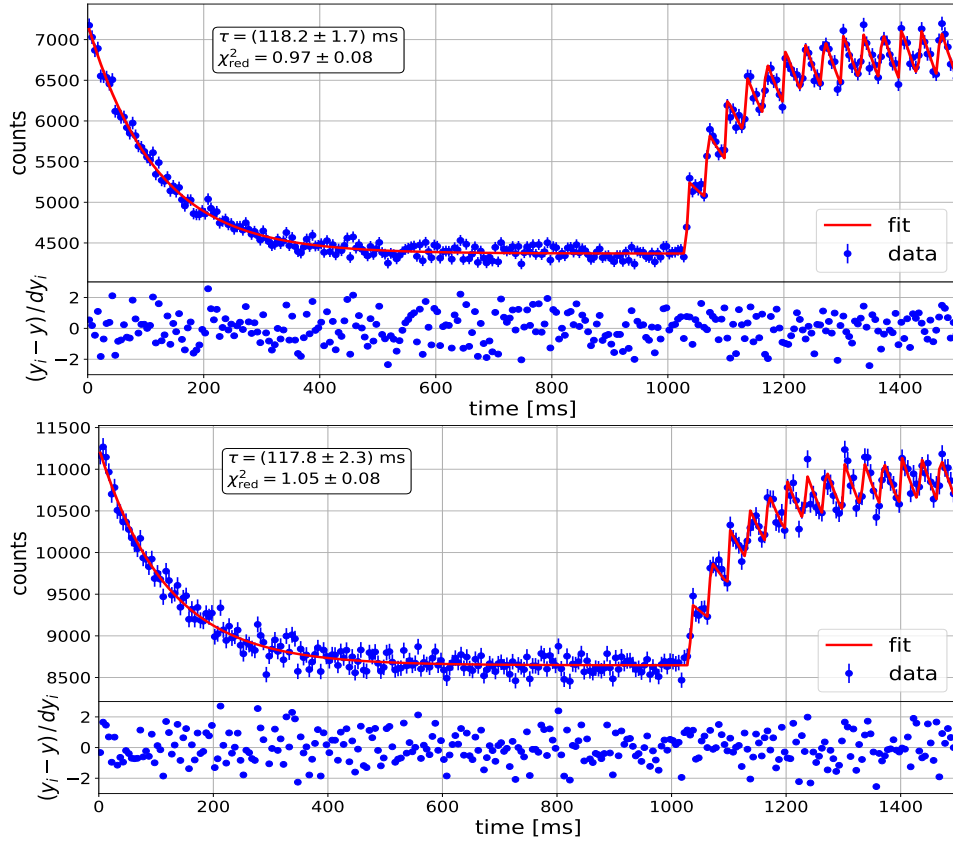


**Figure 4.** Accumulated data for the lifetime of the upper HFS state in  $^{209}\text{Bi}^{80+}$  taken before (top) and after (bottom) the electron cooler maintenance. The data is fitted with the model described in section 3.2 taking the laser pulse structure into account for times larger 1000 ms.

extracted lifetimes of both datasets are consistent with each other and with fit results obtained from the first 1000 ms of the data, where only the exponential decay is observed (see table 1).

**Table 1.** Fit results for  $Li$ -like bismuth lifetimes as observed in the laboratory frame before and after the maintenance, using only the exponentially decaying part of the lifetime curve (0-1000 ms) or the complete datasets (0-1500 ms). The uncertainties are purely statistical.

Fit interval	0 - 1000 ms	0 - 1500 ms
before maintenance	$(118.3 \pm 2.1) \text{ ms}$	$(118.2 \pm 1.7) \text{ ms}$
after maintenance	$(118.5 \pm 3.2) \text{ ms}$	$(117.8 \pm 2.3) \text{ ms}$
weighted mean	$(118.4 \pm 1.8) \text{ ms}$	$(118.1 \pm 1.4) \text{ ms}$

*H-like bismuth* For  $H$ -like bismuth the relevant measurements were performed after the repair and we are therefore dealing with one dataset only. Figure 5 displays the accumulated data together with the corresponding fit result delivering a value for the lifetime of the upper HFS state in  $^{209}\text{Bi}^{82+}$  of  $(566.7 \pm 2.2) \mu\text{s}$  in the laboratory frame.



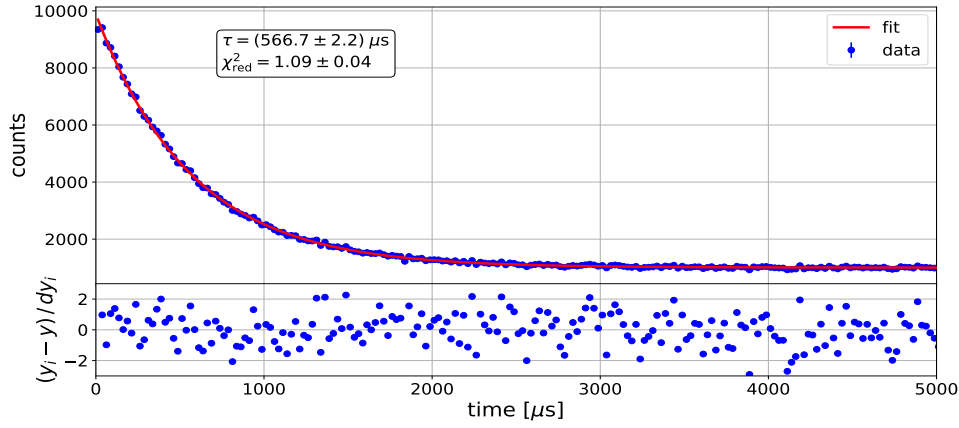


**Figure 5.** Accumulated data for the lifetime of the upper HFS state in  $^{209}\text{Bi}^{82+}$ . The data is fitted by an exponential function with a constant background term.

### 3.4. Systematic uncertainties

A number of measurements were performed to investigate possible systematic effects on the measured wavelengths of the HFS transitions in  $^{209}\text{Bi}^{82+}$  and  $^{209}\text{Bi}^{80+}$  [4, 7]. By selecting from these runs only those periods when the laser was on resonance, we can also perform checks of systematic effects on the lifetime of the HFS states, albeit with very restricted statistics. Figure 6 displays the results of these investigations for the lifetime of the upper HFS state in  $Li$ -like bismuth. To investigate possible effects of space charge

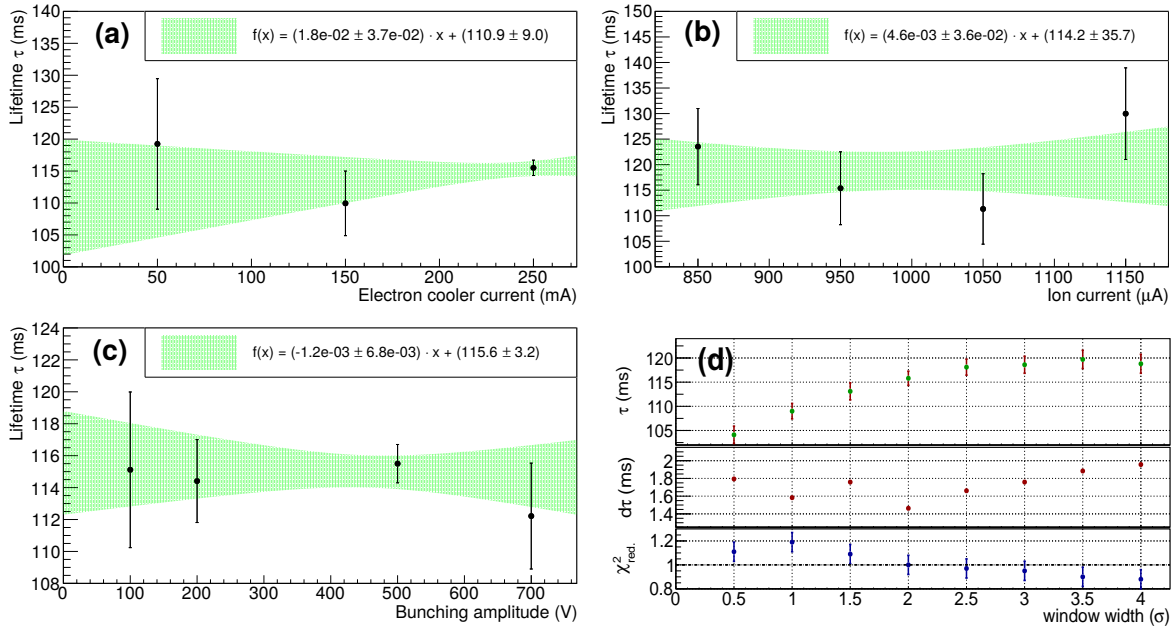


**Figure 6.** Investigation of systematic uncertainties for the lifetime of the upper HFS state in  $Li$ -like bismuth. (a) dependence of the extracted lifetime on electron cooler current, (b) the ion current and (c) the bunching amplitude. Plots (a-c) were produced using a  $2\sigma$  summation window. (d) dependence of the extracted lifetime on the width of the summation window used to construct the lifetime curves.

of the electron beam generated by the cooler or of the ion beam itself, lifetimes have been extracted for different values of the electron cooler current and the ion current (figure 6, (a) and (b)). Additionally a series of measurements were taken with different amplitudes of the RF buncher voltage that is used to concentrate the ions stored inside the ESR into two bunches (figure 6, (c)). The green bands illustrate  $1\sigma$  uncertainty intervals of linear fits applied to the corresponding displayed data points. Within the uncertainties the slopes of all three fits are compatible with zero and, therefore, none of the described measurements displayed a systematic change of the lifetime with the respective experimental parameters. The same findings apply to the systematic tests of the lifetime of the upper HFS state in  $^{209}\text{Bi}^{82+}$ .

A systematic uncertainty arising in the analysis of the experimental data is given by the chosen width of the analysis window used to sum up the counts in the signal peaks of the individual bunch histograms (see figure 2). Choosing a too small window leads to shifts in the observed lifetimes as the widths of the signal peaks has been found to slightly fluctuate over the decay period [16]. Choosing a too large window on the other hand results in an increased fit uncertainty and a lesser quality of the fit demonstrated by a reduced  $\chi^2$ -value that starts to significantly deviate from one. The effect of a systematic variation of the width of the analysis window from  $\pm 0.5\sigma$  to  $\pm 4\sigma$  is displayed in figure 6 (d), for the Li-like dataset before the cooler maintenance. It can be seen that for small window widths the lifetime of the state is underestimated but stabilizes when moving to larger widths. The optimum value chosen for the analysis is  $\pm 2.5\sigma$ , where the lifetime has already reached the plateau, the uncertainty of the fit value is comparably small and the reduced  $\chi^2$  compatible with one. To estimate the systematical uncertainty connected to this analysis procedure, we calculate the differences between the lifetimes derived with  $\pm 2\sigma$ ,  $\pm 2.5\sigma$  and  $\pm 3\sigma$  width of the analysis window. The weighted mean of these differences is then taken as systematic uncertainty of the analysis of the given dataset. The systematic uncertainty for the lifetime of the upper HFS state in  $^{209}\text{Bi}^{82+}$  was calculated accordingly.

Overall we arrive at the following lifetimes for the upper HFS states in  $^{209}\text{Bi}^{82+}$  and  $^{209}\text{Bi}^{80+}$  in the laboratory system:

$$\tau_{\text{lab}}(^{209}\text{Bi}^{82+}) = (566.7 \pm 2.2_{\text{stat.}} \pm 1.3_{\text{sys.}}) \mu\text{s} \quad (7)$$

$$\tau_{\text{lab}}(^{209}\text{Bi}^{80+}) = (118.1 \pm 1.4_{\text{stat.}} \pm 1.3_{\text{sys.}}) \text{ms} . \quad (8)$$

### 3.5. Lifetimes in the rest frame of the ions

To transform the measured lifetimes from the laboratory frame to the rest frame of the ions we need to know the respective velocities of the ions. In the experiment the ion velocity is determined by the velocity of the electrons in the cooler, which itself can be calculated from the acceleration voltage applied to the cooler and space-charge corrections taking into account a reduction of the potential felt by the electrons due to shielding effects in the electron beam. To determine the latter, several measurements were conducted with H-like ion beams during which the electron cooler current was

varied and the cooler voltage subsequently adjusted to achieve a constant revolution frequency of the ions in the ring. From a linear fit to the obtained data points, the space-charge correction was found to be  $(-0.162 \pm 0.009) \text{ V/mA}$  [7]. The average voltage during the lifetime measurements extracted from the datasets and corrected for the space-charge effect is for the case of H-like bismuth found to be  $U_{\text{eff}}(^{209}\text{Bi}^{82+}) = (-213878 \pm 9) \text{ V}$  and for Li-like bismuth  $U_{\text{eff}}(^{209}\text{Bi}^{80+}) = (-213871 \pm 10) \text{ V}$  (the latter value has been obtained from the datasets after the cooler maintenance). Besides the uncertainties of the space charge correction the quoted error bars include the standard deviation of the high voltage measurements from the calculated mean (1.3 V for  $^{209}\text{Bi}^{82+}$  and 2.1 V for  $^{209}\text{Bi}^{80+}$ ), the uncertainty of the scale factor of the PTB HVDC voltage divider (13 ppm [17]) and uncertainties due to the difference in contact potentials of cathode and drift tubes of the electron cooler ( $\leq 3 \text{ V}$ ). For a conservative estimate of the overall uncertainty on the effective cooler voltage  $U_{\text{eff}}$  these contributions were added linearly.

We can then calculate the Lorentz factor using

$$\gamma = 1 + \frac{e U_{\text{eff}}}{m_e c^2} \quad (9)$$

with the electron charge  $e$  and electron rest mass  $m_e$  to obtain  $\gamma(^{209}\text{Bi}^{82+}) = 1.418548(18)$  and  $\gamma(^{209}\text{Bi}^{80+}) = 1.418534(20)$ . With these results the measured lifetimes can be transferred into the laboratory system using  $\tau = \tau_{\text{lab}}/\gamma$  yielding the results listed in table 2. The values are in excellent agreement with the theoretical predictions in both

**Table 2.** Results for the lifetimes of the upper HFS state in  $^{209}\text{Bi}^{82+}$  and  $^{209}\text{Bi}^{80+}$  compared to existing experimental and theoretical data.

	H-like bismuth $^{209}\text{Bi}^{82+}$	Li-like bismuth $^{209}\text{Bi}^{80+}$
this work	$(399.5 \pm 1.6_{\text{stat.}} \pm 0.9_{\text{sys.}}) \mu\text{s}$	$(83.3 \pm 1.0_{\text{stat.}} \pm 0.9_{\text{sys.}}) \text{ ms}$
H. Winter et al. (exp.) [11, 12]	$(397.5 \pm 1.5_{\text{stat.}}) \mu\text{s}$	
I. Klaft et al. (exp.) [18]	$(351 \pm 16_{\text{stat.}}) \mu\text{s}$	
V.M. Shabaev (theo.) [19]	$(399.01 \pm 0.19) \mu\text{s}$	
V.M. Shabaev et al. (theo.) [14]		$(82.0 \pm 1.4) \text{ ms}$
Calculated from theoretical $g$ -factor [20] and wavelength [21]		$(82.85 \pm 0.61) \text{ ms}$

cases. Our measurement of the lifetime of the HFS state in  $^{209}\text{Bi}^{82+}$  agrees within the uncertainties with the previous measurement by Winters et al. [11, 12] while excluding the older value of Klaft et al. [18].

#### 4. Extraction of the $g$ -factors

From the measured transition energies [4] and lifetimes of the HFS states one can extract the  $g$ -factors of the bound  $1s$  electron for H-like bismuth and the  $g$ -factor of the bound  $2s$  electron for Li-like bismuth.

The transition probability between the ground state hyperfine states of  $^{209}\text{Bi}^{82+}$ , including first order QED and nuclear corrections, can be written as [19, 22]:

$$\frac{1}{\tau} = \frac{\alpha}{3\hbar} \frac{\Delta E_{\text{HFS}}^3}{(m_e c^2)^2} \frac{I}{2I+1} \left[ g_e - g_I \frac{m_e}{m_p} \right]^2, \quad (10)$$

where  $\Delta E_{\text{HFS}}$  is the experimentally determined transition energy of the HFS state,  $I$  is the nuclear spin ( $I = \frac{9}{2}$  for  $^{209}\text{Bi}$ ),  $g_e$  is the bound-electron  $g$ -factor and  $g_I$  is the nuclear  $g$ -factor. The last term can be written as

$$g_I \cdot \frac{m_e}{m_p} = \frac{m_e}{m_p} \cdot \frac{\mu_{\text{Bi}}}{\mu_N} \quad (11)$$

with  $\mu_{\text{Bi}}$  being the magnetic moment of  $^{209}\text{Bi}$  and  $\mu_N$  the nuclear magneton. This magnetic moment has recently been re-measured [23] yielding a value of

$$\mu_{\text{Bi}} = (4.092 \pm 0.002) \cdot \mu_N. \quad (12)$$

Together with the experimental HFS splitting of  $\Delta E_{\text{HFS}}(^{209}\text{Bi}^{82+}) = 5.08503(2)(9) \text{ eV}$  [4] this leads to a  $g_e$ -factor for the 1s electron in H-like bismuth of

$$g_e^{\text{exp}}(^{209}\text{Bi}^{82+}) = 1.7294 \pm 0.0035_{\text{stat.}} \pm 0.0019_{\text{sys.}} \quad (13)$$

in good agreement to the theoretical calculation performed in [24] which yields

$$g_e^{\text{theo}}(^{209}\text{Bi}^{82+}) = 1.731014 \pm 0.000001. \quad (14)$$

Equation 10 can also be applied for the calculation of the bound electron  $g$ -factor in Li-like ions from the experimentally determined lifetime and energy splitting. With the experimentally determined transition energy of  $\Delta E_{\text{HFS}}(^{209}\text{Bi}^{80+}) = 0.797645(4)(14) \text{ eV}$  [4] and the lifetime presented in this work, the experimentally determined  $g_e$ -factor for the 2s electron in lithium-like bismuth is found to be:

$$g_e^{\text{exp}}(^{209}\text{Bi}^{80+}) = 1.928 \pm 0.012_{\text{stat.}} \pm 0.010_{\text{sys.}}, \quad (15)$$

in good agreement to the theoretical value determined from [25]

$$g_e^{\text{theo}}(^{209}\text{Bi}^{80+}) = 1.934739 \pm 0.000003. \quad (16)$$

## 5. Summary

The lifetimes of the upper HFS states in  $^{209}\text{Bi}^{82+}$  and, for the first time, in  $^{209}\text{Bi}^{80+}$  have been measured by the LIBELLE experiment and are compared to previous experimental and/or theoretical results. Except for an older measurement of the lifetime in H-like bismuth by Klaft et al. [18] all results agree within the respective uncertainties. Using the lifetimes extracted in this work and the energy splittings derived from the same experiment by Ullmann et al. [4] it is possible to calculate  $g$ -factors of the bound 1s electron for H-like bismuth and of the bound 2s electron for Li-like bismuth. Also here the results obtained are in good agreement with theoretical predictions.

In the near future, it is foreseen to extend the measurements of the specific difference of the HFS transition energies as well as the lifetimes and  $g$ -factors to the isotopic chain in bismuth. A first candidate for these investigations will be  $^{208}\text{Bi}$ , whose nuclear magnetic moment has been recently measured [26].

## Acknowledgments

This work was supported by the German Federal Ministry of Education and Research (BMBF) under grant numbers 05P12PMFAE, 05P15PMFAA, 05P12RDFA4, 05P12R6FAN and 05P15RGFAA. The work was further supported by the Helmholtz International Centre for FAIR (HIC for FAIR) within the LOEWE program by the federal state Hessen. M.L., C.T. and J.U. acknowledge support from HGS-HiRe.

We appreciate technical support during the beam time by F. Nolden, C. Dimopoulou, J. Rossbach, and D. Winters and the GSI accelerator department. We also thank S. Minami and N. Kurz for their support in the development of the data acquisition system and R. Jöhren for his earlier contributions to the data acquisition and the mirror system.

## References

- [1] V. M. Shabaev et al., *Stringent tests of QED using highly charged ions*, Hyperfine Interactions 239 (2018) 60
- [2] H. Persson et al., *A theoretical survey of QED tests in highly charged ions*, Hyperfine Interactions 108 (1997) 3
- [3] V. M. Shabaev et al., *Towards a Test of QED in Investigations of the Hyperfine Splitting in Heavy Ions*, Phys. Rev. Lett. 86 (2001) 3959
- [4] J. Ullmann et al., *High precision hyperfine measurements in Bismuth challenge bound-state strong-field QED theory*, Nature Communications 8 (2017) 15484
- [5] R. Snchez et al., *Laser spectroscopy measurement of the 2s-hyperfinesplitting in lithium-like bismuth*, J. Phys. B 50 (2017) 085004
- [6] R. Snchez et al., *Hyperfine transition in  $^{209}\text{Bi}^{80+}$  - one step forward*, Phys. Scripta T166 (2015) 014021
- [7] J. Ullmann et al., *An improved value for the hyperfine splitting of hydrogen-like  $^{209}\text{Bi}^{82+}$* , J. Phys. B: At. Mol. Opt. Phys. 48 (2015) 144022
- [8] J. Vollbrecht et al., *Laser spectroscopy of the ground-state hyperfine structure in H-like and Li-like bismuth*, J. Phys.: Conf. Ser. 583 (2015) 012002
- [9] M. Lochmann et al., *Observation of the hyperfine transition in lithium-like bismuth  $^{209}\text{Bi}^{80+}$  : Towards a test of QED in strong magnetic fields*, Phys. Rev. A 90 (2014) 030501(R)
- [10] W. Nörtershäuser et al., *First Observation of the Ground-State Hyperfine Transition in  $^{209}\text{Bi}^{80+}$* , Phys. Scripta T156 (2013) 014016
- [11] H. Winter et al., *Bound Electron  $g$ -Factor in Hydrogen-Like Bismuth*, GSI Scientific Report 1998, GSI Report 1999-1 (1999) 87
- [12] H. Winter, *Laserspektroskopie an schweren Ionen: Laserinduzierte Zweistufen-Rekombination, Hyperfeinstrukturaufspaltung und  $g$ -faktor des gebundenen Elektrons*, Dissertation, TU Darmstadt, 1999.
- [13] P. Seelig et al., *Ground State Hyperfine Splitting of Hydrogenlike  $^{207}\text{Pb}^{81+}$  by Laser Excitation of a Bunched Ion Beam in the GSI Experimental Storage Ring*, Phys. Rev. Lett. 81 (1998) 4824
- [14] V.M. Shabaev et al., *Transition energy and lifetime for the ground-state hyperfine splitting of high- $Z$  lithiumlike ions*, Phys. Rev. A 58 (1998) 1610
- [15] V. Hannen et al., *Detection system for forward emitted photons at the Experimental Storage Ring at GSI*, JINST 8 (2013) P09018 , (arXiv:1305.4069)
- [16] J. Vollbrecht, *Lifetime analysis of the HFS states in hydrogen- and lithium-like bismuth and development of an in-beam detection system for extreme UV photons*, Dissertation, University of Münster, 2016

- [17] J. Hällström et al., *Performance of a Wideband 200-kV HVDC Reference Divider Module*, IEEE Transactions on Instrumentation and Measurement 63 (2014) 2264-2270
- [18] I. Klaft et al., *Precision Laser Spectroscopy of the Ground State Hyperfine Splitting of Hydrogenlike  $^{209}\text{Bi}^{82+}$* , Phys. Rev. Lett. 73 (1994) 2425
- [19] V.M. Shabaev, *Transition probability between the hyperfine structure components of hydrogenlike ions and bound-electron g-factor*, Canadian Journal of Physics 76 (1998) 907-910
- [20] D.L. Moskovkin et al., *g factor of Li-like ions with a nonzero nuclear spin*, Optics and Spectroscopy 104 (2008) 637649
- [21] A.V. Volotka et al., *Test of Many-Electron QED Effects in the Hyperfine Splitting of Heavy High-Z Ions*, Phys. Rev. Lett. 108 (2012) 073001
- [22] T. Beier et al.,  *$g_j$  factor of an electron bound in a hydrogenlike ion*, Phys. Rev. A 62 (2000) 032510
- [23] L.V. Skripnikov et al., *New Nuclear Magnetic Moment of  $^{209}\text{Bi}$ : Resolving the Bismuth Hyperfine Puzzle*, Phys. Rev. Lett. 120 (2018) 093001
- [24] D.L. Moskovkin et al., *g factor of hydrogenlike ions with nonzero nuclear spin*, Phys. Rev. A 70 (2004) 032105
- [25] D.L. Moskovkin et al., *g Factor of Li-like Ions with a Nonzero Nuclear Spin*, Optics and Spectroscopy 104 (2008) 637649.
- [26] S. Schmidt et al., *The nuclear magnetic moment of  $^{208}\text{Bi}$  and its relevance for a test of bound-state strong-field QED*, Phys. Lett. B 779 (2018) 324-330